CORRECTION

Mutations in *TOP3A* Cause a Bloom Syndrome-like Disorder

Carol-Anne Martin, Kata Sarlós, Clare V. Logan, Roshan Singh Thakur, David A. Parry, Anna H. Bizard, Andrea Leitch, Louise Cleal, Nadia Shaukat Ali, Mohammed A. Al-Owain, William Allen, Janine Altmüller, Miriam Aza-Carmona, Bushra A.Y. Barakat, Jimena Barraza-García, Amber Begtrup, Massimo Bogliolo, Megan T. Cho, Jaime Cruz-Rojo, Hassan Ali Mundi Dhahrabi, Nursel H. Elcioglu, GOSgene, Gráinne S. Gorman, Rebekah Jobling, Ian Kesterton, Yoshihito Kishita, Masakazu Kohda, Polona Le Quesne Stabej, Asam Jassim Malallah, Peter Nürnberg, Akira Ohtake, Yasushi Okazaki, Roser Pujol, Maria José Ramirez, Anya Revah-Politi, Masaru Shimura, Paul Stevens, Robert W. Taylor, Lesley Turner, Hywel Williams, Carolyn Wilson, Gökhan Yigit, Laura Zahavich, Fowzan S. Alkuraya, Jordi Surralles, Alejandro Iglesias, Kei Murayama, Bernd Wollnik, Mehul Dattani, Karen E. Heath, Ian D. Hickson,* and Andrew P. Jackson*

(The American Journal of Human Genetics *103*, 221–231; August 2, 2018)

In this paper, the mutation at the cDNA level for individuals P9 and P10 is stated as c.2771dup, when it should be as stated for individuals P2–P4, P6, c.2271dup. The protein consequence is stated correctly. The authors regret the error.

*Correspondence: iandh@sund.ku.dk (I.D.H.), andrew.jackson@igmm.ed.ac.uk (A.P.J.)

Mutations in *TOP3A* Cause a Bloom Syndrome-like Disorder

Carol-Anne Martin,[1,26] Kata Sarlós,[2,26] Clare V. Logan,[1,26] Roshan Singh Thakur,[2,26] David A. Parry,[1] Anna H. Bizard,[2] Andrea Leitch,[1] Louise Cleal,[1] Nadia Shaukat Ali,[3] Mohammed A. Al-Owain,[4] William Allen,[5] Janine Altmüller,[6] Miriam Aza-Carmona,[7,8] Bushra A.Y. Barakat,[3] Jimena Barraza-García,[7,8] Amber Begtrup,[9] Massimo Bogliolo,[8,10] Megan T. Cho,[9] Jaime Cruz-Rojo,[11] Hassan Ali Mundi Dhahrabi,[3] Nursel H. Elcioglu,[12] GOSgene,[13] Gráinne S. Gorman,[14] Rebekah Jobling,[15] Ian Kesterton,[16] Yoshihito Kishita,[17] Masakazu Kohda,[17] Polona Le Quesne Stabej,[13] Asam Jassim Malallah,[3] Peter Nürnberg,[6] Akira Ohtake,[18] Yasushi Okazaki,[17] Roser Pujol,[8,10] Maria José Ramirez,[8,10] Anya Revah-Politi,[19] Masaru Shimura,[20] Paul Stevens,[16] Robert W. Taylor,[14] Lesley Turner,[21] Hywel Williams,[13] Carolyn Wilson,[5] Gökhan Yigit,[22] Laura Zahavich,[15] Fowzan S. Alkuraya,[23,27] Jordi Surralles,[8,10,24,27] Alejandro Iglesias,[25,27] Kei Murayama,[20,27] Bernd Wollnik,[22,27] Mehul Dattani,[13,27] Karen E. Heath,[7,8,27] Ian D. Hickson,[2,*] and Andrew P. Jackson[1,*]

Bloom syndrome, caused by biallelic mutations in *BLM*, is characterized by prenatal-onset growth deficiency, short stature, an erythematous photosensitive malar rash, and increased cancer predisposition. Diagnostically, a hallmark feature is the presence of increased sister chromatid exchanges (SCEs) on cytogenetic testing. Here, we describe biallelic mutations in *TOP3A* in ten individuals with prenatal-onset growth restriction and microcephaly. *TOP3A* encodes topoisomerase III alpha (TopIIIα), which binds to BLM as part of the BTRR complex, and promotes dissolution of double Holliday junctions arising during homologous recombination. We also identify a homozygous truncating variant in *RMI1*, which encodes another component of the BTRR complex, in two individuals with microcephalic dwarfism. The *TOP3A* mutations substantially reduce cellular levels of TopIIIα, and consequently subjects' cells demonstrate elevated rates of SCE. Unresolved DNA recombination and/or replication intermediates persist into mitosis, leading to chromosome segregation defects and genome instability that most likely explain the growth restriction seen in these subjects and in Bloom syndrome. Clinical features of mitochondrial dysfunction are evident in several individuals with biallelic *TOP3A* mutations, consistent with the recently reported additional function of TopIIIα in mitochondrial DNA decatenation. In summary, our findings establish *TOP3A* mutations as an additional cause of prenatal-onset short stature with increased cytogenetic SCEs and implicate the decatenation activity of the BTRR complex in their pathogenesis.

Introduction

Microcephalic primordial dwarfism (MPD) is used to collectively describe a heterogeneous group of disorders characterized by significant in utero and postnatal growth retardation alongside marked microcephaly.[1] Bloom syndrome (MIM: 210900) is also associated with prenatal growth restriction, short stature, and microcephaly. It is distinguished by an erythematous sun-sensitive facial rash that can become evident during childhood.[2] A predisposition to the development of cancer in early adulthood is also seen, and both solid tumors and hematological malignancies are a major cause of early death.[3] Additionally, a key cytogenetic feature of Bloom syndrome is an increased number of sister chromatid exchanges (SCEs).[4] Notably, when

[1]MRC Human Genetics Unit, MRC Institute of Genetics and Molecular Medicine, University of Edinburgh, Edinburgh EH4 2XU, UK; [2]Center for Chromosome Stability and Center for Healthy Aging, Department of Cellular and Molecular Medicine, University of Copenhagen, Blegdamsvej 3B, 2200 Copenhagen N, Denmark; [3]Dubai Hospital, Al Khaleej Street, Al Baraha, PO Box 7272, Dubai; [4]Department of Medical Genetics, King Faisal Specialist Hospital and Research Center, Riyadh 11211, Saudi Arabia; [5]Fullerton Genetics Center, Asheville, NC 28803, USA; [6]Cologne Center for Genomics, University of Cologne, 50931 Cologne, Germany; [7]Institute of Medical and Molecular Genetics and Skeletal dysplasia multidisciplinary Unit, Hospital Universitario La Paz, Universidad Autónoma de Madrid, IdiPaz, Madrid 28046, Spain; [8]Centro de Investigación Biomédica en Red de Enfermedades Raras, Madrid 28029, Spain; [9]GeneDx, 207 Perry Parkway, Gaithersburg, MD 20877, USA; [10]Department of Genetics and Microbiology, Universitat Autònoma de Barcelona, Bellaterra 08193, Spain; [11]Department of Pediatric Endocrinology & Dysmorphology, Hospital 12 Octubre, Madrid 28041, Spain; [12]Department of Pediatric Genetics, Marmara University Medical School, Istanbul 34722, Turkey; [13]UCL Great Ormond Street Institute of Child Health, 30 Guilford Street, London WC1N 1EH, UK; [14]Wellcome Centre for Mitochondrial Research, Institute of Neuroscience, School of Medical Education, Newcastle University, Newcastle upon Tyne NE2 4HH, UK; [15]The Hospital for Sick Children, Toronto, ON M5G 1X8, Canada; [16]Cytogenetics Department, Viapath Analytics, Guy's Hospital, London SE1 9RT, UK; [17]Intractable Disease Research Center, Graduate School of Medicine, Juntendo University, 2-1-1, Hongo, Bunkyo-ku, Tokyo 113-8421, Japan; [18]Department of Pediatrics, Faculty of Medicine, Saitama Medical University, 38 Morohongo, Moroyama, Saitama 350-0495, Japan; [19]Institute for Genomic Medicine, Columbia University Medical Center, New York, NY 10032, USA; [20]Center for Medical Genetics, Department of Metabolism, Chiba Children's Hospital, 579-1, Heta-cho, Midori-ku, Chiba 266-0007, Japan; [21]Memorial University of Newfoundland, St. John's, NL A1C 5S7, Canada; [22]Institute of Human Genetics, University Medical Center Göttingen, 37073 Göttingen, Germany; [23]Department of Genetics, King Faisal Specialist Hospital and Research Center, Riyadh 11211, Saudi Arabia; [24]Department of Genetics and Biomedical Research Institute Sant Pau, Hospital de la Santa Creu i Sant Pau, Barcelona 08041, Spain; [25]Department of Pediatrics, Division of Clinical Genetics, Columbia University Medical Center, New York, NY 10032, USA
[26]These authors contributed equally to this work
[27]These authors contributed equally to this work
*Correspondence: iandh@sund.ku.dk (I.D.H.), andrew.jackson@igmm.ed.ac.uk (A.P.J.)
https://doi.org/10.1016/j.ajhg.2018.07.001

molecular testing is inconclusive, a finding of elevated SCEs is currently utilized for diagnostic confirmation of Bloom syndrome (see GeneReviews in Web Resources).

In 1995, Bloom syndrome was shown to be caused by mutations in *BLM* (MIM: 604610), which encodes a RecQ family DNA helicase.[5] Mutations in *BLM* are typically biallelic loss-of-function mutations.[6] BLM forms the BTRR complex with topoisomerase III alpha (TopIIIα) and RecQ-mediated genome instability proteins 1 and 2 (RMI1 and RMI2, respectively). Together, these proteins process double Holliday junctions (dHJs) that arise as a result of homologous-recombination-mediated repair of double-stranded DNA (dsDNA) breaks during DNA synthesis.[7–13] The process of dHJ dissolution requires two steps. First, the BTRR complex promotes the convergent branch migration of the dHJ to create a hemicatenane intermediate, and then this structure is decatenated by TopIIIα in concert with RMI1 and RMI2.[14,15] Dissolution of a dHJ by this mechanism can be completed without any potentially detrimental exchanges between genetic markers flanking the original site of homologous recombination. The alternative processing of dHJs by Holliday junction resolvases (SLX-MUS81 and GEN1 nucleases) can yield crossover events, and increased usage of this pathway has been proposed to explain the increase in SCEs in BLM-deficient cells.[16] Crossover events between homologous chromosomes can lead to loss of heterozygosity (LOH),[17] which can be detrimental to cell survival and contribute to increased cancer predisposition.[18] Additionally, unresolved recombination intermediates can persist into mitosis, leading to chromosome bridges, and act as a source of genome instability.[19]

Here, we report the identification of pathogenic mutations in *TOP3A* (MIM: 601243) in ten individuals with Bloom syndrome-like phenotypic features and characterize the cellular consequences of these mutations.

Material and Methods

Research Subjects
Genomic DNA from the affected individuals and family members was extracted from peripheral blood by standard methods or obtained from saliva samples with Oragene collection kits according to the manufacturer's instructions. Informed consent was obtained from all participating families, and all procedures performed in studies involving human participants were in accordance with the Declaration of Helsinki. Research studies were approved by the Scottish Multicenter Research Ethics Committee (05/MRE00/74), the Hospital Universitario La Paz Ethical Committee (PI-2630), the Great Ormond Street Hospital Research Ethics Committee (09/H0706/66), the University Medical Center Göttingen Ethics Committee (vote ref. 3/2/1), and the Institute for Genomic Medicine at Columbia University (protocol AAAO8410).

Parents provided written consent for the publication of photographs of the affected individuals. For growth measurements, *Z* scores (standard deviations from population mean for age and sex) were calculated according to LMS (L, smooth curve; M, median; S, coefficient of variation) growth on the basis of British 1990 growth reference data.[20] For calculation of *Z* scores for growth measurements published for Bloom syndrome,[21] full-term gestation was assumed, and postnatal growth measurements were calculated from data provided for the 18- to 21-year age range.

Exome Sequencing and Sanger Sequencing
Exome sequencing and confirmatory capillary Sanger sequencing were performed according to standard methodologies as previously published.[22,23] TOP3A and RMI1 variants were annotated with GenBank: NM_004618.4 and NM_024945.2 reference sequences, respectively.

Plasmid Construct and Protein Purification
Cloning of the Mutant hTopIIIα Expression Vector
A plasmid encoding the wild-type (WT) *TOP3A* cDNA[24] was modified by the Quickchange XL Site-Directed Mutagenesis Kit (Agilent technologies) with the following primers to recapitulate the deletion and frameshift present in subject P1: 5′-CCCTCCGTCACAC GACTGTGCAGAAGGA-3′ (T3_FS_FW) and 5′-TCCTTCTGCACA GTCGTGTGACGGAGGG-3′ (T3_FS_RW).
Expression and Purification of TRR
The previously described plasmids encoding RMI1 and RMI2[13] and hTopoIIIα[24] were co-transformed into *E. coli* Rosetta 2 cells, and the complex was expressed. The cells were disrupted in buffer A (50 mM Tris-HCl [pH 7.5], 0.5 M NaCl, 10% glycerol, 0.1% IGEPAL, 2 mM β-mercaptoethanol, 40 mM imidazole, 1 mM PMSF, and protease inhibitor tablet [PI, EDTA-free, Roche]) on ice before dounce homogenization and sonication. After the removal of cell debris by centrifugation, the lysate was affinity purified on a 5 mL HisTrap HP affinity column. The complex was further purified on a 5 mL HiTrap Heparin HP column in buffer B (50 mM Tris-HCl [pH 7.5], 10% glycerol, 0.1 mM EDTA, and 1 mM DTT) with a linear gradient of 200 mM to 1 M NaCl and then gel filtered on a 120 mL HiLoad 16/600 Superdex 200 column in buffer B containing 200 mM NaCl. Expression and purification of the mutant T^{Thr812LeufsTer101}RR complex were performed in a similar manner. BLM was purified as described previously.[25,26]
dHJ Dissolution
The dHJ substrate construction and dissolution reactions were carried out as described previously.[14]

Cell Culture
Dermal fibroblasts were obtained by skin-punch biopsy and were maintained in amnioMAX C-100 complete medium (Life Technologies) in a 37°C incubator with 5% CO_2 and 3% O_2. siRNA oligonucleotides (siLUC: 5′-CUUACGCUGAGUACUUCGA-3′ [siTopIIIα SMARTpool M-005279-01-0005, Dharmacon]) were transfected into dermal fibroblasts with RNAiMAX (Life Technologies) according to the manufacturer's instructions.

Sister Chromatid Exchange Assay
Dermal fibroblasts were treated with 10 μM BrdU for 48 hr followed by 0.5 μg/mL colcemid for 2 hr. Metaphases and nuclei were isolated in hypotonic buffer (0.25% KCl and 1% $Na_3C_6H_5O_7$), fixed with methanol and acetic acid (3:1 vol/vol), and dropped onto slides. Dried slides were rehydrated in PBS and then incubated with 2 μg/mL Hoescht 33342 stain in 2× saline sodium citrate (SSC) buffer (300 mM NaCl and 30 mM sodium citrate) for 15 min. Slides were then covered in 2× SSC buffer,

Table 1. Identified *TOP3A* and *RMI1* Variants Associated with Microcephalic Dwarfism

Family	Individual	Gene	Biallelic Nucleotide Mutations	Predicted Amino Acid Consequence(s)	Sex	Country of Origin
1	P1	*TOP3A*	c.[2718del];[2718del]	p.[Thr907LeufsTer101];[Thr907LeufsTer101]	female	USA (Czech and Irish ancestry)
2	P2	*TOP3A*	c.[2271dup];[2271dup]	p.[Arg758GlnfsTer3];[Arg758GlnfsTer3]	female	United Arab Emirates
	P3	*TOP3A*	c.[2271dup];[2271dup]	p.[Arg758GlnfsTer3];[Arg758GlnfsTer3]	female	United Arab Emirates
	P4	*TOP3A*	c.[2271dup];[2271dup]	p.[Arg758GlnfsTer3];[Arg758GlnfsTer3]	male	United Arab Emirates
3	P5	*TOP3A*	c.[527C>T];[1072_1073dup][a]	p.[Ala176Val];[Tyr359GlyfsTer17]	female	Japan
4	P6	*TOP3A*	c.[2271dup];[2271dup]	p.[Arg758GlnfsTer3];[Arg758GlnfsTer3]	female	Syria
5	P7	*TOP3A*	c.[2428del];[2428del]	p.[Ser810LeufsTer2];[Ser810LeufsTer2]	female	Spain
	P8	*TOP3A*	c.[2428del];[2428del]	p.[Ser810LeufsTer2];[Ser810LeufsTer2]	male	Spain
6	P9	*TOP3A*	c.[2771dup];[2771dup]	p.[Arg758GlnfsTer3];[Arg758GlnfsTer3]	male	Syria
7	P10	*TOP3A*	c.[2771dup];[2771dup]	p.[Arg758GlnfsTer3];[Arg758GlnfsTer3]	female	Saudi Arabia
8	P11	*RMI1*	c.[1255_1259del];[1255_1259del]	p.[Lys419LeufsTer5]; [Lys419LeufsTer5]	female	Turkey
	P12	*RMI1*	c.[1255_1259del];[1255_1259del]	p.[Lys419LeufsTer5];[Lys419LeufsTer5]	female	Turkey
–	MC1[b]	*TOP3A*	c.[298A>G];[403C>T]	p.[Met100Val];[Arg135Ter]	female	UK

Nomenclature is according to transcript GenBank: NM_004618.4 for *TOP3A* and GenBank: NM_004618.4 and NM_024945.2 for *RMI1*.
[a]Close to donor splice site of exon 10.
[b]Previously reported individual with adult-onset mitochondrial disease.[32]

irradiated in ultraviolet A at 5,400 J/m^2, dehydrated in an ethanol series, and mounted in VECTASHIELD with DAPI.

SCE Methodology for Analysis of P7 and P8
Dermal fibroblasts were treated with 26.05 μM BrdU for 72 hr followed by 0.5 μg/mL colcemid for 5 hr and then harvested. Cells were resuspended in a pre-warmed hypotonic solution (0.051 M KCl) for 20 min at 37°C, fixed with methanol and acetic acid (3:1 vol/vol), and dropped onto slides. Samples were aged for at least 3 days and then stained with 1.56 μg/mL Hoechst 33258 (Sigma, B2883). Slides were irradiated in 2× SSC with ultraviolet C (356 nm) at 0.260 J/cm^2, washed with 2× SSC, and stained with 10% Giemsa in phosphate buffer.

SCE analysis of peripheral-blood samples was performed according to standard methodology in a diagnostic lab setting.[27]

Immunofluorescence and microscopy
Mitotic abnormalities and G1-associated defects were analyzed as described previously.[28,29] In brief, for mitotic analysis, cells were seeded onto 22 × 22 mm glass coverslips in 6-well plates. After 18 hr, cells were treated with 3.5 μM RO3306 for 6 hr for the induction of a late G2 arrest and were subsequently released into fresh media. After 45 min, cells were fixed with 4% paraformaldehyde containing 0.2% Triton X-100 in PBS for 20 min. For G1-associated defects, RO3306-treated cells were released into fresh media for 30 min. Prometaphase cells were shaken off and re-seeded onto glass slides coated with poly-L-lysine. After 4–6 hr, cells were fixed with 4% paraformaldehyde for 10 min and permeabilized with 0.5% Triton X-100 for 10 min. Fixed cells were incubated with antibodies specific to cyclin A (Santa Cruz Biotechnology, sc-596), 53BP1 (Santa Cruz Biotechnology, sc-515841), and PICH.[30]

Immunoblotting
Cells were lysed in 50 mM Tris-HCl (pH 8), 280 mM NaCl, 0.5% NP40, 0.2 mM EDTA, 0.2 mM EGTA, and 10% glycerol supple-mented with a protease inhibitor tablet (Roche Life Science). Protein samples were run on a 4%–12% NuPAGE Bis-Tris precast gel (Life Technologies) and then immunoblotted with anti-TopIIIα raised against amino acids 652–1,001 (Proteintech, 14525-1-AP) and actin (Sigma, A2066).

Results

Identification of Mutations in *TOP3A*
In ongoing work to identify genes associated with microcephalic dwarfism, whole-exome sequencing (WES) was performed on subject P1, who had significant microcephaly and short stature (−5.7 and −4.4 standard deviations [SD], respectively). This identified the homozygous frameshift mutation c.2718del (p.Thr907LeufsTer101) (GenBank: NM_004618.4) in *TOP3A* in chromosomal region 17p11.2. After interrogation of other cohorts and clinical contacts made through GeneMatcher,[31] we subsequently ascertained a further nine individuals from seven families affected by biallelic deleterious *TOP3A* variants that had also been discovered by WES (Table 1). All variants identified were validated by Sanger capillary sequencing, and all parents were confirmed to be heterozygous carriers. Aside from the c.2718del variant (minor allele frequency = 0.00041%), none of the other variants were reported in GnomAD.[33] Notably, four of the families from the United Arab Emirates, Syria, and Saudi Arabia (F2, F4, F6, and F7), were homozygous for the same variant.

Prenatal-Onset Growth Restriction and Microcephaly in Individuals with *TOP3A* Mutations
Prenatal growth restriction was evident from the substantially reduced birth weight in all individuals (mean weight

Table 2. Growth Parameters of Individuals with *TOP3A* and *RMI1* Mutations

Individual	Mutated Gene	Birth							Postnatal						
			Weight		OFC		Length			Weight		OFC		Height	
		Gestational Age (Weeks)	kg	Z Score (SD)[a]	cm	Z Score (SD)	cm	Z Score (SD)	Age at Exam	kg	Z Score (SD)[a]	cm	Z Score (SD)	cm	Z Score (SD)
P1	*TOP3A*	37	1.35	−3.9	27.5	−4.2	38	−5.4	5 months	4.9	−2.7	36	−5.7	54.8	−4.4
P2	*TOP3A*	37	1.9	−2.3	NA	NA	NA	NA	3 years	9.5	−3.7	47.5	−2.3	84.5	−2.8
P3	*TOP3A*	37	2.2	−1.6	NA	NA	NA	NA	8 years	16.5	−3.3	49.5	−2.9	112.5	−2.7
P4	*TOP3A*	40	2.2	−2.9	NA	NA	NA	NA	10 years	18.1	−4.6	49.5	−3.1	113	−4.1
P5	*TOP3A*	35	1.91	−1.3	31.8	−0.2	43	−1.8	15 years	20	−6.4	51	−3.1	138	−3.7
P6	*TOP3A*	NA	2	NA	NA	NA	NA	NA	19 months	5.17	−7.5	44.3	−3.0	64.3	−5.8
P7	*TOP3A*	38	1.90	−2.8	30.0	−2.7	41	−4.1	3 years, 3 months	7.21	−7.0	44.2	−5.3	78.7	−4.7
P8	*TOP3A*	34	1.41	−2.5	28.5	−2.2	42	−2.1	7 years[b]	10	−2.9	45.8	−5.0	98.1	−4.5
P9	*TOP3A*	40	2	−3.4	NA	NA	NA	NA	11 years	21.6	−3.5	47.5	−4.5	125.6	−2.7
P10	*TOP3A*	36	1.6	−2.7	NA	NA	NA	NA	4 years, 7 months	9	−6.1	45.5	−5.0	91	−3.3
P11	*RMI1*	34	1.59	−1.7	NA	NA	NA	NA	7 years	14	−3.8	46.5	−5	100	−4
P12	*RMI1*	38	1.80	−3.1	NA	NA	NA	NA	13 years	39	−0.9	48	−5	135	−2.9
MC1[c]	*TOP3A*	NA	NA	NA	NA	NA	NA	NA	adult	NA	NA	NA	NA	163	NA

Z scores are the standard deviation from population mean for age and sex. The following abbreviation is used: NA, not available.
[a]Adjusted for gestation.
[b]Growth-hormone treatment from 4 years, 3 months of age to 5 years, 11 months of age showed no response.
[c]Previously reported individual with adult-onset mitochondrial disease (ataxia and progressive external ophthalmoplegia).[32]

−2.6 ± 0.9 SD; Table 2 and Figure 1A). Postnatally, weight (mean −4.8 ± 1.8 SD), height (mean −3.9 ± 1.0 SD), and occipital-frontal circumference (mean −4.0 ± 1.2 SD) were significantly reduced. Growth parameters were similar to those previously reported for Bloom syndrome (mean birth weight −3.7 ± 1.2 SD, mean postnatal weight −3.8 ± 2.1 SD, and mean height −3.9 ± 1.1 SD).[21] Although multiple café-au-lait patches were present in some individuals with *TOP3A* mutations, the classical erythematous malar facial rash was not apparent, and there were no reports of malignancies (although none had yet reached adulthood; Table 3 and Figure 1B).

Cardiomyopathy Is Present in Some Individuals with *TOP3A* Mutations

A single individual compound heterozygous for rare *TOP3A* variants has been reported recently with an adult-onset mitochondrial disorder (denoted as MC1 in Table 1).[32] Whereas stature was normal (163 cm) in this adult female, several of the subjects reported here had clinical features that could also be attributable to mitochondrial dysfunction. P3 and P4 (family 2) had an additional diagnosis of dilated cardiomyopathy, which proved fatal in P4 at age 10 years. Another brother in this sibship died as a result of cardiomyopathy at the age of 13 years. Morphometric and other clinical information are not available for this individual. In P5 (family 3), a dilated cardiomyopathy was also reported, and skeletal muscle biopsy demonstrated 87% mitochondrial DNA depletion. P8 also had asymptomatic left ventricular dilatation
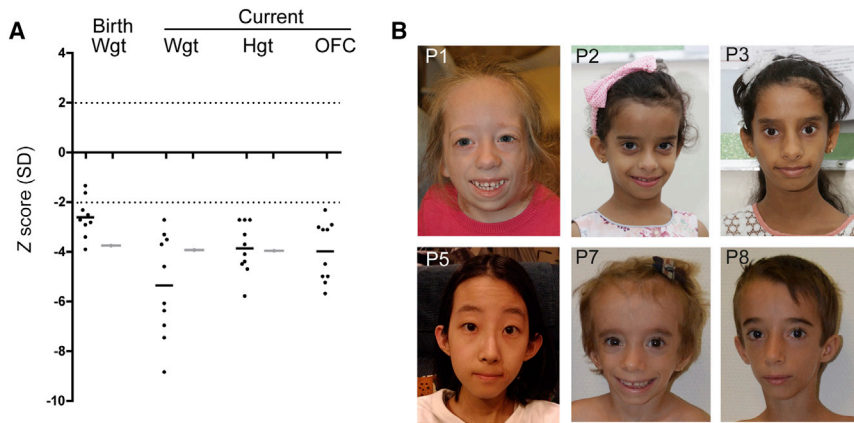
noted on echocardiography, whereas P9 had hypertrophic cardiomyopathy.

Given the identification of multiple individuals with biallelic deleterious variants in *TOP3A*, alongside a consistent clinical phenotype across the cohort, we concluded that these mutations were likely to be pathogenic. We therefore pursued confirmatory functional studies by employing both biochemical and cell-biological approaches.

TOP3A Mutations Lead to Markedly Reduced Cellular Amounts of Enzyme TopIIIα

Most of the identified *TOP3A* mutations are predicted to prematurely truncate the encoded protein (Figure 2A) and hence are likely to have significant effects on cellular protein amounts. We therefore assessed the amounts of TopIIIα in primary dermal fibroblast cell lines derived from P1, P7, and P8. Immunoblotting demonstrated that the amount of full-length TopIIIα was substantially lower in total cell lysates from all three individuals than in cell lines from unrelated control individuals and parents (Figure 2B).

In most subjects, the frameshift mutations would be expected to result in nonsense-mediated decay of *TOP3A* transcripts, explaining the consequent loss of TopIIIα. However, the homozygous frameshift mutation in P1 (c.2718del [p.Thr907LeufsTer101]) is at the 3′ end of the gene and is not predicted to result in NMD; instead, it would result in a protein with a length similar to that of the WT enzyme. The frameshift did, however, result in abolition of the C-terminal zinc-finger domain, whose precise cellular function remains to be defined. We therefore

expressed recombinant TopIIIα[Thr907LeufsTer101] in *E. coli* and purified it to homogeneity as a complex with the co-expressed RMI1 and RMI2 in order to characterize it further. Notably, in contrast to the TRR complex containing TopIIIα[WT], the complex containing TopIIIα[Thr907LeufsTer101] (hereafter referred to as TopIIIα[P1]) exhibited reduced stability during purification; lower yields and increased amounts of degraded products were evident on SDS-PAGE (Figure 2C). Nevertheless, when used in quantities equimolar to those of TopIIIα[WT], TopIIIα[P1] was proficient in a biochemical assay for dHJ dissolution when combined with other components of the BTRR complex. This indicates that this TopIIIα variant retains a near-normal level of single-stranded DNA (ssDNA) decatenation activity (Figures 2D–2F). Therefore, we concluded that the major consequence of the TopIIIα[P1] variant, like the other truncating variants, is severe depletion of TopIIIα enzymatic activity in cells.

P5 was the only individual we identified to have an amino acid substitution, p.Ala176Val, that was present *in trans* with a frameshift mutation. This amino acid substitution is absent from GnomAD, and *in silico* analyses (MutationTaster, CADD, and SIFT) predict it to be deleterious. It is at a highly conserved residue (Figure S1) within the TOPA domain (Figure 2A) and would therefore be expected to be highly deleterious to enzymatic function.

Given the above results and that *Top3a* is a developmentally essential gene in mice,[34] we conclude that all of the identified mutations result in marked but most likely hypomorphic loss of function of TopIIIα as a result of a reduction in the cellular amount of the protein. Therefore, these mutations would be predicted to severely compromise the decatenation activity of the BTRR complex in dHJ dissolution *in vivo*. To assess this possibility, we next pursued cellular assays to assess SCE frequency.

SCEs Are Markedly Elevated in Individuals with *TOP3A* Mutations

dHJ can be processed by two pathways; first, dissolution by the BTRR complex yields non-crossover products only; second, resolution by endonucleases that cleave Holliday junctions generate both non-crossovers and crossover products that are visualized as SCEs (Figure 3A). To determine if dHJ dissolution is impaired in the cells of affected individuals, we assessed the frequency of SCEs. After BrdU incorporation, we performed differential sister chromatid staining on primary fibroblasts and PHA-stimulated peripheral blood leukocytes (Figures 3B and 3C). Cells from individuals with *TOP3A* mutations had substantially (3- to 6-fold) more SCEs, than cells from control individuals or heterozygous parents (p < 0.0001 for all affected individual cell lines; Figure 3C). Therefore, excessive crossover recombination was evident in all tested individuals with *TOP3A* mutations, indicating that diagnostic cytogenetic assessment of SCE levels is predictive of *TOP3A* mutations as well as *BLM* mutations.

Chromosome Segregation Defects and Genome Instability Occur in Cells with *TOP3A* Mutations

Impaired dHJ decatenation can result in persistently entangled sister chromatids that impede chromosome segregation at mitosis.[19] Therefore, we performed detailed characterization of the mitotic consequences of TopIIIα deficiency in primary fibroblasts from P1. DAPI staining demonstrated elevated amounts of chromatin bridges (control [C] = 0, parent = 0.3 ± 0.4, and P1 = 4 ± 0.6) and lagging chromatin and chromosomes (C = 0.9 ± 0.2, parent = 4 ± 0.7, and P1 = 9.2 ± 0.9) (Figures 4A and 4B), consistent with persisting chromosome entanglements. Additionally, increased numbers of ultrafine DNA bridges (UFBs) were revealed by immunostaining for PICH on DAPI-negative regions[19] (C = 2.7 ± 0.3, parent = 13.1 ± 1.1, and P1 = 26.7 ± 3.8).

We then examined the post-mitotic consequences of the observed chromosome segregation errors by enriching for G1 cells (Figures 4C and 4D). Micronuclei often arise from chromosome segregation errors,[35] and analysis of DAPI-stained cells demonstrated substantially more micronucleated cells in the P1 fibroblast cell line than in control and parental cell lines (C = 0.4 ± 0.2, parent = 1.8 ± 0.5,

Table 3. Clinical Phenotype of Individuals with *TOP3A* and *RMI1* Mutations

	TOP3A											*RMI1*	
	P1	P2	P3	P4	P5	P6	P7	P8	P9	P10	MC1	P11	P12
Age	5 months	3 years	8 years	10 years	15 years	19 months	3 years	7 years	11 years	4 years, 7 months	adult	7 years	13 years
Prenatal-onset growth restriction	yes	yes	yes	yes	yes	yes	yes	yes	yes	yes	no	yes	yes
Elevated sister chromatid exchange	yes	yes	yes	NA	yes	NA	yes	yes	yes	NA	no	NA	NA
Café-au-lait macules	yes	yes	yes	yes	no	yes	no	yes	yes	yes	NA	no	no
Developmental delay	mild	no	no	no	no	mild[a]	no	mild	no	mild	NA	mild	no
Cancer[b]	no	no	no	no	no	no	no	no	no	no	NA	no	no
Decreased subcutaneous fat	no	no	no	no	no	no	yes	yes	no	yes	NA	no	no
Gastroesophageal reflux	yes	NA	NA	NA	no	yes	no	NA	no	NA	NA	no	no
Diabetes mellitus	no	no	no	no	no	no	no	no	no	no	NA	no	no
Recurrent infections	yes[c]	NA	NA	NA	no	no	no	NA	yes	yes[d]	NA	no	no
Malar rash	no	no	no	no	no	no	no	no	no	no	NA	no	no
Dilated cardiomyopathy	no	no	yes	yes (severe, deceased)	yes (after heart transplant)	normal echocardiogram	NA	yes[e] (asymptomatic)	HCM	no	NA	NA	NA
Mitochondrial DNA depletion in muscle	NA	NA	NA	N/A	yes (87%)	NA	NA	NA	NA	NA	yes (>80%)	NA	NA
Other	CDH, gastrostomy	no	abnormal movements and tics	no	hearing loss, CMAMMA	no	no	no	microcytic anemia[f]	no	PEO, ataxia	no	no

Abbreviations are as follows: CDH, Congenital dislocation of hip; CMAMMA, combined malonic and methylmalonic aciduria (MIM: 614265) due to *ACSF3* (MIM: 614245) mutations; HCM, hypertrophic cardiomyopathy; NA, not available; and PEO, progressive external ophthalmoplegia.
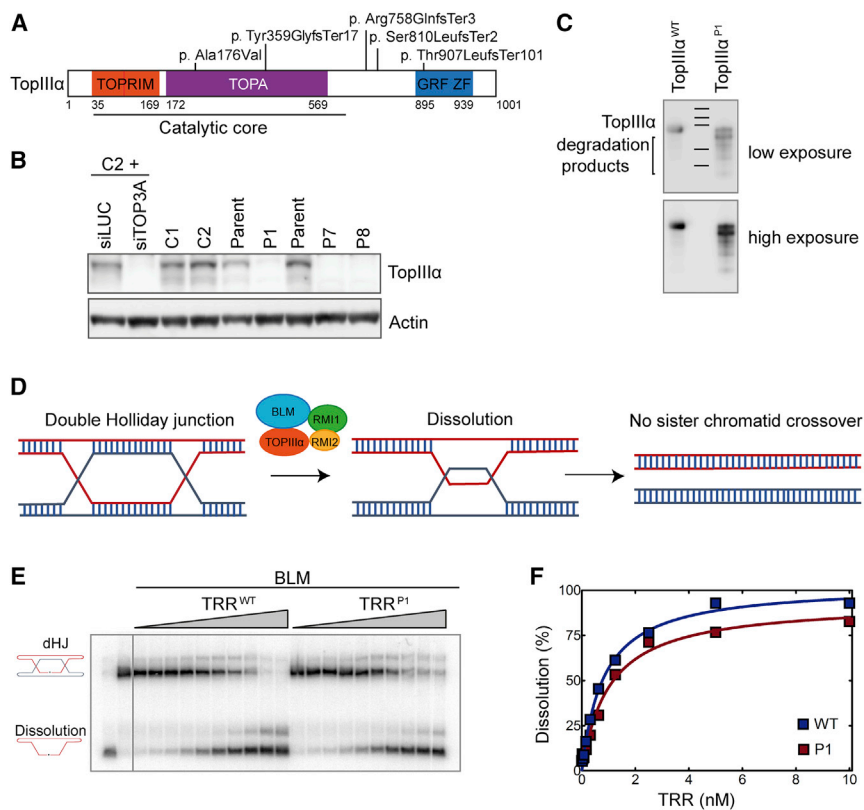[a]Expressive speech delay only.
[b]All individuals are younger than 15 years old; in Bloom syndrome, neoplasia typically manifests in early adulthood.
[c]Recurrent otitis media and tonsillitis, leading to tonsillectomy.
[d]Reccurent upper-respiratory-tract infections and oral thrush.
[e]Mild left-ventricle dilatation.
[f]Anemia due to beta-thalassemia trait.

Figure 2. Mutations in *TOP3A* Markedly Reduce Amounts of TopIIIα but Do Not Affect Its Intrinsic Decatenation Activity

(A) Schematic of TopIIIα with locations of variants annotated. Colors are as follows: red, TOPRIM domain; purple, TOPA domain; and blue, GRF zinc-finger domain.

(B) *TOP3A* mutations markedly reduce protein amounts. An immunoblot of a polyacrylamide gel is shown and was generated from total cell lysates from dermal fibroblast lines derived from affected individuals probed with an anti-TopIIIα antibody. siRNA depletion of TOP3A in a fibroblast line from control 2 was used to confirm the specificity of the antibody. C1 and C2 are unrelated control fibroblast lines. TopIIIα antibody was raised against amino acids 652–1,001.

(C) Recombinant TopIIIα[Thr812LeufsTer101] (denoted TopIIIα[P1]) is less stable than TopIIIα[WT]. An immunoblot of a polyacrylamide gel is shown and was generated from purified TopIIIα[WT] and TopIIIα[P1] proteins probed with an anti-TopIIIα antibody. Protein size markers are 250, 170, 140, 100, and 70 kDa.

(D) Schematic depicting the BTRR complex and its role in dHJ dissolution. Homologous sister chromatids are shown in red and blue.

(E and F) TopIIIα[P1] is proficient for promoting dHJ dissolution with BLM in combination with RMI1 and RMI2. (E) Representative polyacrylamide gel demonstrating the enzyme-concentration dependence of the dHJ dissolution activity of TopIIIα[WT] and mutant (TopIIIα[P1]) TRR complexes with 20 nM BLM at 37°C in 30 min. TRR was included in reactions at increasing concentrations ranging from 20 pM to 10 nM. A labeled circular oligonucleotide (lane 1) and dHJ (lane 2) were included as markers. (F) Quantification of the dHJ dissolution reaction shown in (E). The reaction was repeated twice more with very similar results.

and P1 = 7.5 ± 1.4). Elevated amounts of 53BP1 nuclear bodies were also seen in cyclin-A-negative (G1) cells, indicating the transmission of DNA damage from one cell cycle to the next[36] (C = 0.8 ± 0.3, parent = 4.5 ± 0.5, and P1 = 11 ± 1.7). Altogether, we conclude that impaired dHJ decatenation in TopIIIα-deficient cells results in both abnormal recombination and mitotic errors that lead to accumulation of DNA damage. Because chromatin bridges and UFBs are also present in individuals affected by Bloom syndrome,[19] these findings are concordant with a shared disease mechanism.

A Homozygous Truncating Variant in *RMI1* Is Associated with Microcephalic Dwarfism

Finally, through WES we also identified the homozygous truncating variant c.1255_1259del (p.Lys419Leufs*5) in *RMI1* in two affected cousins (P11 and P12) from a consanguineous Turkish family (F8; Table 1 and Figure S3). Both individuals also had microcephalic dwarfism with a clinical phenotype and level of growth restriction similar to those of individuals with *TOP3A* mutations (Figure 1A and Tables 2 and 3).

Discussion

Here, we report that biallelic mutations in *TOP3A* cause prenatal growth restriction, microcephaly, and short stature, a clinical phenotype overlapping that seen in Bloom syndrome. Furthermore, we have identified a rare *RMI1* truncating variant (allele frequency = 1.1 × 10^{−5}) in two individuals. Given that no homozygous loss-of-function variants are reported in gnomAD, we expect this to be the cause of microcephalic dwarfism in individuals P11 and P12. However, it will be necessary to identify more individuals with other deleterious sequence variants to establish *RMI1* as a disease-related gene.

Notably, individuals with *TOP3A* mutations exhibit elevated amounts of SCEs on cytogenetic testing. Although cell lines were not available from P11 and P12, we also predict that increased SCEs will occur in cells with the homozygous RMI1 p.Lys419Leufs*5 variant given the important role of this protein in the BTRR complex.[9,10,37] For many years, the diagnosis of Bloom syndrome rested on a demonstration of elevated SCEs, and this has continued to be employed in cases where molecular testing is inconclusive (see GeneReviews in Web Resources). Hence, analysis of other BTRR components is now warranted when elevated SCEs are detected. Indeed, given the clear phenotypic overlap between Bloom syndrome and individuals with *TOP3A* mutations, re-evaluation of individuals previously cytogenetically diagnosed with Bloom syndrome could be fruitful.
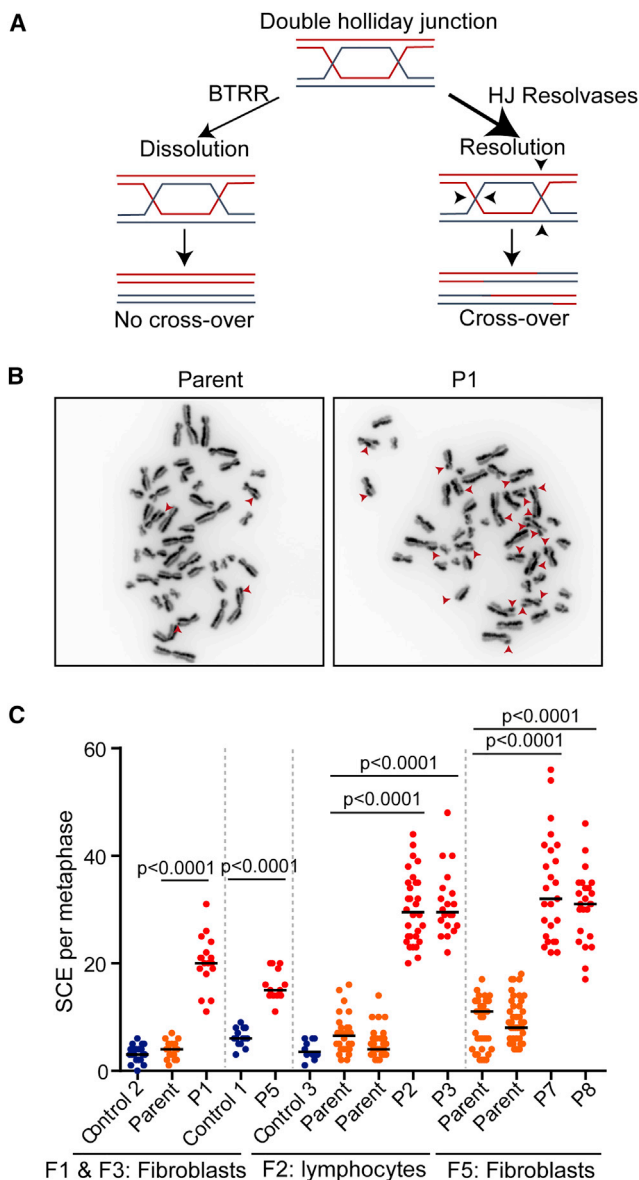
Figure 3. Individuals with *TOP3A* Mutations Have More SCEs, Reflecting Chromatid Hyper-recombination

(A) Schematic of dHJ processing. dHJs are either dissolved by the BTRR complex or alternatively cleaved by structure-specific nucleases that lead to dHJ resolution.

(B and C) BrdU strand-specific labeling of sister chromatids shows that TOP3A cells have more SCEs than control and parent cells. (B) Representative images of P1 and parent fibroblast cell lines. (C) Quantification of SCEs in fibroblast cell lines (P1, P5, P7, and P8) or PHA-stimulated lymphocytes derived from peripheral-blood samples (P2 and P3). The median value was plotted with more than ten metaphase spreads counted per subject. Pairwise non-parametric Mann Whitney tests were performed against parental control cells. F1, F2, and F5 SCEs were scored in independent laboratories.

RMI2 is the fourth component of the BTRR complex. A single family in which two children were also found to have elevated SCEs was recently reported to have a homozygous deletion of *RMI2*; café-au lait macules were evident, but only one individual showed mild-

growth impairment.[38] Because RMI2 is not essential for BTR (BLM, TopIIIα, and RMI1) enzymatic function,[12] a more subtle cellular and developmental phenotype might therefore result. It also remains possible that the BTR complex has functions independent of RMI2 given that BLM, TopIIIα, and RMI1 are conserved in all eukaryotes but RMI2 is absent in invertebrates and yeast.[13]

Bloom syndrome is associated with a predisposition to both solid tumors and hematological malignancies.[3] However, cancers have not been reported in our individuals with *TOP3A* mutations. Nevertheless, all are still children, and because malignancy in Bloom syndrome typically manifests in early adulthood, *TOP3A* mutations could also confer an increased risk of neoplasia.

Distinct from Bloom syndrome, some of our individuals with *TOP3A* mutations have clinical features consistent with mitochondrial dysfunction, and several exhibit a dilated cardiomyopathy. Notably, an individual with chronic progressive external ophthalmoplegia and cerebellar ataxia, along with a novel functional role for TopIIIα in the decatenation of mitochondrial DNA after its replication, has been recently reported[32] (denoted as subject MC1). The compound-heterozygous mutations c.[298A>G];[403C>T], p.[Met100Val];[Arg135*] could have milder consequences than those reported in our cohort, and consistent with this, we found that MC1 does not exhibit short stature (Table 2) or elevated numbers of SCEs in a primary fibroblast line derived from this individual (Figure S2). Thus, it appears that the residual TopIIIα activity in MC1 is sufficient for the nuclear function of the BTRR complex in dHJ dissolution and for normal growth but could have become rate limiting for the role of TopIIIα in mitochondrial DNA replication.

Mechanistically, our cellular and biochemical studies suggest that the identified *TOP3A* mutations reported here are severe hypomorphs, consistent with the established essential cellular and developmental functions of TopIIIα.[34] Given that marked growth restriction is common in individuals with *TOP3A* and *BLM* mutations, it seems likely that they have a shared pathogenic basis arising from reduced ssDNA decatenation activity of the BTRR complex. Persistence of unresolved hemicatenanes into mitosis leads to the formation of chromatin and ultrafine mitotic bridges that have previously been reported in Bloom syndrome[19] and in individuals with microcephalic dwarfism and condensin mutations.[39] The resulting genome instability arising from persistent chromatin bridges[40,41] and micronuclei[42] could therefore impair cell viability during development, causing microcephaly and global growth restriction. In summary, we demonstrate that mutations in *TOP3A* cause microcephalic dwarfism with increased SCE, implicating the BTRR complex as a cause of growth disorders.
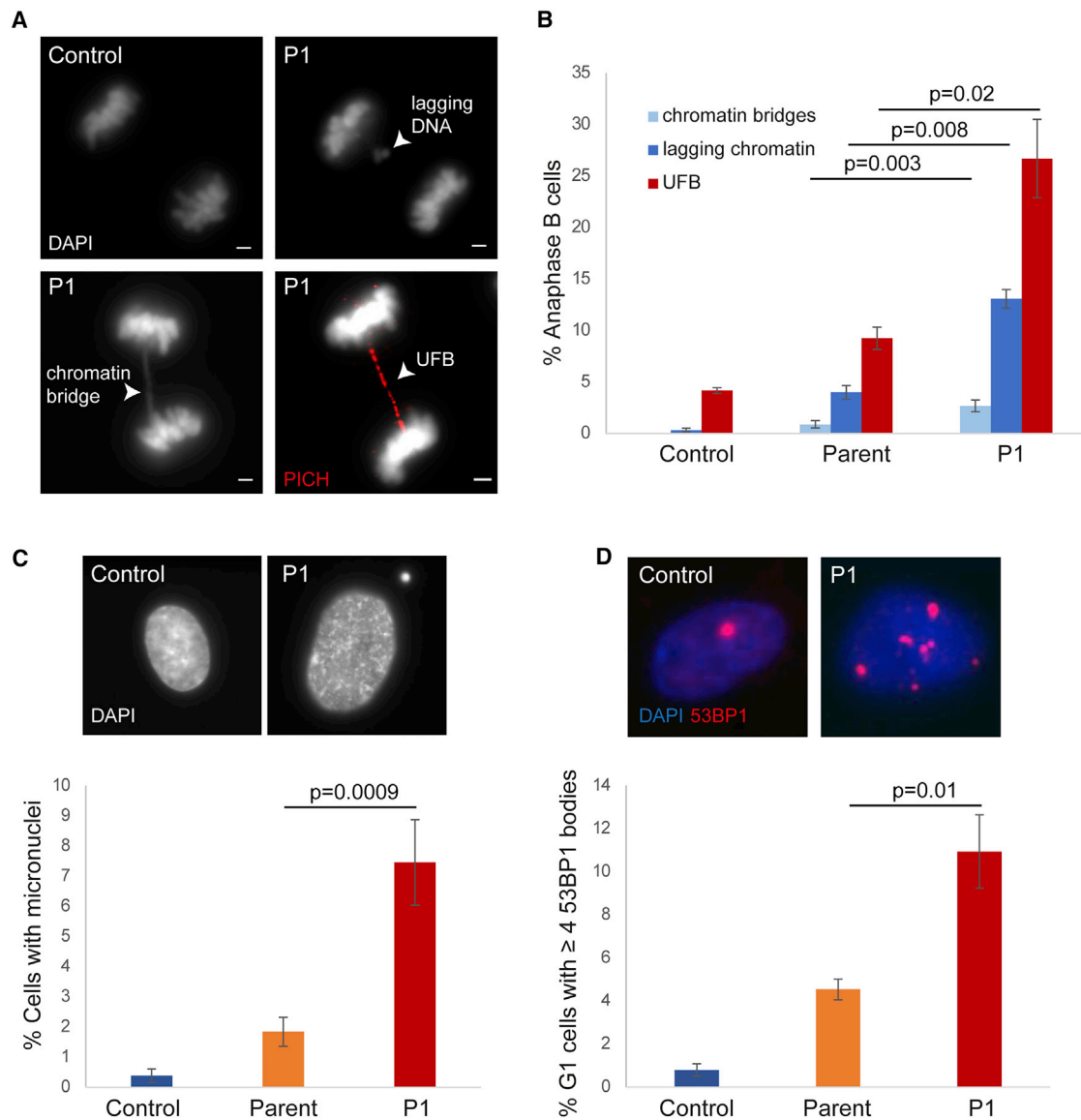
Figure 4. DNA Catenanes Persist into Mitosis in Cells with *TOP3A* Mutations, Leading to Chromosome Segregation Defects and Genome Instability

(A and B) Chromosome segregation is impaired in *TOP3A*-deficient primary fibroblasts. (A) Representative images of chromatin bridges, lagging DNA (DAPI), and UFBs (detected by the presence of PICH and absence of DAPI stain). (B) Quantification of chromatin bridges, lagging DNA, and PICH-positive UFBs scored in control, parental, and P1 mitotic fibroblasts staged at anaphase B (experiments ≥ 3, n > 50 cells, error bars = SEM). To enrich for mitotic cells, we treated fibroblasts with R03306 for 6 hr and released and fixed them after 45 min.
(C) *TOP3A* P1 fibroblasts display significantly elevated amounts of micronuclei. Top: representative picture of control and P1 fibroblasts. Bottom: quantification of micronucleus containing interphase cells (experiments ≥ 3, n > 500, error bars = SEM). To enrich for G1 cells, we released RO3306-treated cells into fresh media for 30 min and collected, re-seeded, and fixed prometaphase cells after 4–6 hr.
(D) P1 fibroblasts with *TOP3A* mutations display significantly elevated numbers of 53BP1 bodies in G1 nuclei. Top: representative images of 53BP1 foci (red) and DNA (DAPI). Bottom: quantification of cells with at least four 53BP1 foci in G1 nuclei (negative for cyclin A) (experiments ≥ 3, n > 500, error bars = SEM). Scale bar: 2 microns. Two-tailed t test was performed against parent cells.

Supplemental Data

Acknowledgments

Declaration of Interests

Web Resources

GenBank, https://www.ncbi.nlm.nih.gov/genbank/

GeneReviews, Sanz, M.M., German, J., and Cunniff, C. (1993). Bloom's Syndrome, https://www.ncbi.nlm.nih.gov/books/NBK1398/

GnomAD, http://gnomad.broadinstitute.org

OMIM, http://www.omim.org

References

1. Klingseisen, A., and Jackson, A.P. (2011). Mechanisms and pathways of growth failure in primordial dwarfism. Genes Dev. *25*, 2011–2024.

2. Bloom, D. (1954). Congenital telangiectatic erythema resembling lupus erythematosus in dwarfs; probably a syndrome entity. AMA Am. J. Dis. Child. *88*, 754–758.

3. German, J. (1997). Bloom's syndrome. XX. The first 100 cancers. Cancer Genet. Cytogenet. *93*, 100–106.

4. Chaganti, R.S., Schonberg, S., and German, J. (1974). A manyfold increase in sister chromatid exchanges in Bloom's syndrome lymphocytes. Proc. Natl. Acad. Sci. USA *71*, 4508–4512.

5. Ellis, N.A., Groden, J., Ye, T.Z., Straughen, J., Lennon, D.J., Ciocci, S., Proytcheva, M., and German, J. (1995). The Bloom's syndrome gene product is homologous to RecQ helicases. Cell *83*, 655–666.

6. German, J., Sanz, M.M., Ciocci, S., Ye, T.Z., and Ellis, N.A. (2007). Syndrome-causing mutations of the BLM gene in persons in the Bloom's Syndrome Registry. Hum. Mutat. *28*, 743–753.

7. Johnson, F.B., Lombard, D.B., Neff, N.F., Mastrangelo, M.A., Dewolf, W., Ellis, N.A., Marciniak, R.A., Yin, Y., Jaenisch, R., and Guarente, L. (2000). Association of the Bloom syndrome protein with topoisomerase IIIalpha in somatic and meiotic cells. Cancer Res. *60*, 1162–1167.

8. Wu, L., Davies, S.L., North, P.S., Goulaouic, H., Riou, J.F., Turley, H., Gatter, K.C., and Hickson, I.D. (2000). The Bloom's syndrome gene product interacts with topoisomerase III. J. Biol. Chem. *275*, 9636–9644.

9. Raynard, S., Bussen, W., and Sung, P. (2006). A double Holliday junction dissolvasome comprising BLM, topoisomerase IIIalpha, and BLAP75. J. Biol. Chem. *281*, 13861–13864.

10. Wu, L., Bachrati, C.Z., Ou, J., Xu, C., Yin, J., Chang, M., Wang, W., Li, L., Brown, G.W., and Hickson, I.D. (2006). BLAP75/RMI1 promotes the BLM-dependent dissolution of homologous recombination intermediates. Proc. Natl. Acad. Sci. USA *103*, 4068–4073.

11. Yin, J., Sobeck, A., Xu, C., Meetei, A.R., Hoatlin, M., Li, L., and Wang, W. (2005). BLAP75, an essential component of Bloom's syndrome protein complexes that maintain genome integrity. EMBO J. *24*, 1465–1476.

12. Singh, T.R., Ali, A.M., Busygina, V., Raynard, S., Fan, Q., Du, C.H., Andreassen, P.R., Sung, P., and Meetei, A.R. (2008). BLAP18/RMI2, a novel OB-fold-containing protein, is an essential component of the Bloom helicase-double Holliday junction dissolvasome. Genes Dev. *22*, 2856–2868.

13. Xu, D., Guo, R., Sobeck, A., Bachrati, C.Z., Yang, J., Enomoto, T., Brown, G.W., Hoatlin, M.E., Hickson, I.D., and Wang, W. (2008). RMI, a new OB-fold complex essential for Bloom syndrome protein to maintain genome stability. Genes Dev. *22*, 2843–2855.

14. Wu, L., and Hickson, I.D. (2003). The Bloom's syndrome helicase suppresses crossing over during homologous recombination. Nature *426*, 870–874.

15. Plank, J.L., Wu, J., and Hsieh, T.S. (2006). Topoisomerase IIIalpha and Bloom's helicase can resolve a mobile double Holliday junction substrate through convergent branch migration. Proc. Natl. Acad. Sci. USA *103*, 11118–11123.

16. Wechsler, T., Newman, S., and West, S.C. (2011). Aberrant chromosome morphology in human cells defective for Holliday junction resolution. Nature *471*, 642–646.

17. Ajima, J., Umezu, K., and Maki, H. (2002). Elevated incidence of loss of heterozygosity (LOH) in an sgs1 mutant of Saccharomyces cerevisiae: roles of yeast RecQ helicase in suppression of aneuploidy, interchromosomal rearrangement, and the simultaneous incidence of both events during mitotic growth. Mutat. Res. *504*, 157–172.

18. Luo, G., Santoro, I.M., McDaniel, L.D., Nishijima, I., Mills, M., Youssoufian, H., Vogel, H., Schultz, R.A., and Bradley, A. (2000). Cancer predisposition caused by elevated mitotic recombination in Bloom mice. Nat. Genet. *26*, 424–429.

19. Chan, K.L., North, P.S., and Hickson, I.D. (2007). BLM is required for faithful chromosome segregation and its localization defines a class of ultrafine anaphase bridges. EMBO J. *26*, 3397–3409.

20. Cole, T.J., Freeman, J.V., and Preece, M.A. (1998). British 1990 growth reference centiles for weight, height, body mass index and head circumference fitted by maximum penalized likelihood. Stat. Med. *17*, 407–429.

21. Keller, C., Keller, K.R., Shew, S.B., and Plon, S.E. (1999). Growth deficiency and malnutrition in Bloom syndrome. J. Pediatr. *134*, 472–479.

22. Murray, J.E., Bicknell, L.S., Yigit, G., Duker, A.L., van Kogelenberg, M., Haghayegh, S., Wieczorek, D., Kayserili, H., Albert,

M.H., Wise, C.A., et al. (2014). Extreme growth failure is a common presentation of ligase IV deficiency. Hum. Mutat. *35*, 76–85.

23. Tanaka, A.J., Cho, M.T., Millan, F., Juusola, J., Retterer, K., Joshi, C., Niyazov, D., Garnica, A., Gratz, E., Deardorff, M., et al. (2015). Mutations in SPATA5 Are Associated with Microcephaly, Intellectual Disability, Seizures, and Hearing Loss. Am. J. Hum. Genet. *97*, 457–464.

24. Goulaouic, H., Roulon, T., Flamand, O., Grondard, L., Lavelle, F., and Riou, J.F. (1999). Purification and characterization of human DNA topoisomerase IIIalpha. Nucleic Acids Res. *27*, 2443–2450.

25. Karow, J.K., Chakraverty, R.K., and Hickson, I.D. (1997). The Bloom's syndrome gene product is a 3′-5′ DNA helicase. J. Biol. Chem. *272*, 30611–30614.

26. Henricksen, L.A., Umbricht, C.B., and Wold, M.S. (1994). Recombinant replication protein A: expression, complex formation, and functional characterization. J. Biol. Chem. *269*, 11121–11132.

27. Rooney D.E., ed. (2001). Human cytogenetics: Malignancy and acquired abnormalities, Third Edition (Oxford University Press).

28. Bizard, A.H., Nielsen, C.F., and Hickson, I.D. (2018). Detection of Ultrafine Anaphase Bridges. Methods Mol. Biol. *1672*, 495–508.

29. Bhowmick, R., Minocherhomji, S., and Hickson, I.D. (2016). RAD52 Facilitates Mitotic DNA Synthesis Following Replication Stress. Mol. Cell *64*, 1117–1126.

30. Nielsen, C.F., Huttner, D., Bizard, A.H., Hirano, S., Li, T.N., Palmai-Pallag, T., Bjerregaard, V.A., Liu, Y., Nigg, E.A., Wang, L.H., and Hickson, I.D. (2015). PICH promotes sister chromatid disjunction and co-operates with topoisomerase II in mitosis. Nat. Commun. *6*, 8962.

31. Sobreira, N., Schiettecatte, F., Valle, D., and Hamosh, A. (2015). GeneMatcher: a matching tool for connecting investigators with an interest in the same gene. Hum. Mutat. *36*, 928–930.

32. Nicholls, T.J., Nadalutti, C.A., Motori, E., Sommerville, E.W., Gorman, G.S., Basu, S., Hoberg, E., Turnbull, D.M., Chinnery, P.F., Larsson, N.-G., et al. (2018). Topoisomerase 3α Is Required for Decatenation and Segregation of Human mtDNA. Mol. Cell *69*, 9–23.e6.

33. Lek, M., Karczewski, K.J., Minikel, E.V., Samocha, K.E., Banks, E., Fennell, T., O'Donnell-Luria, A.H., Ware, J.S., Hill, A.J., Cummings, B.B., et al.; Exome Aggregation Consortium (2016). Analysis of protein-coding genetic variation in 60,706 humans. Nature *536*, 285–291.

34. Li, W., and Wang, J.C. (1998). Mammalian DNA topoisomerase IIIalpha is essential in early embryogenesis. Proc. Natl. Acad. Sci. USA *95*, 1010–1013.

35. Hoffelder, D.R., Luo, L., Burke, N.A., Watkins, S.C., Gollin, S.M., and Saunders, W.S. (2004). Resolution of anaphase bridges in cancer cells. Chromosoma *112*, 389–397.

36. Lukas, C., Savic, V., Bekker-Jensen, S., Doil, C., Neumann, B., Pedersen, R.S., Grøfte, M., Chan, K.L., Hickson, I.D., Bartek, J., and Lukas, J. (2011). 53BP1 nuclear bodies form around DNA lesions generated by mitotic transmission of chromosomes under replication stress. Nat. Cell Biol. *13*, 243–253.

37. Bocquet, N., Bizard, A.H., Abdulrahman, W., Larsen, N.B., Faty, M., Cavadini, S., Bunker, R.D., Kowalczykowski, S.C., Cejka, P., Hickson, I.D., and Thomä, N.H. (2014). Structural and mechanistic insight into Holliday-junction dissolution by topoisomerase IIIα and RMI1. Nat. Struct. Mol. Biol. *21*, 261–268.

38. Hudson, D.F., Amor, D.J., Boys, A., Butler, K., Williams, L., Zhang, T., and Kalitsis, P. (2016). Loss of RMI2 Increases Genome Instability and Causes a Bloom-Like Syndrome. PLoS Genet. *12*, e1006483.

39. Martin, C.A., Murray, J.E., Carroll, P., Leitch, A., Mackenzie, K.J., Halachev, M., Fetit, A.E., Keith, C., Bicknell, L.S., Fluteau, A., et al.; Deciphering Developmental Disorders Study (2016). Mutations in genes encoding condensin complex proteins cause microcephaly through decatenation failure at mitosis. Genes Dev. *30*, 2158–2172.

40. Janssen, A., van der Burg, M., Szuhai, K., Kops, G.J., and Medema, R.H. (2011). Chromosome segregation errors as a cause of DNA damage and structural chromosome aberrations. Science *333*, 1895–1898.

41. Maciejowski, J., Li, Y., Bosco, N., Campbell, P.J., and de Lange, T. (2015). Chromothripsis and Kataegis Induced by Telomere Crisis. Cell *163*, 1641–1654.

42. Crasta, K., Ganem, N.J., Dagher, R., Lantermann, A.B., Ivanova, E.V., Pan, Y., Nezi, L., Protopopov, A., Chowdhury, D., and Pellman, D. (2012). DNA breaks and chromosome pulverization from errors in mitosis. Nature *482*, 53–58.